European Review for Medical and Pharmacological Sciences 2019; 23: 7722-7731

Accelerated aging effects on color, microhardness and microstructure of ICON resin infiltration

M. CHEN[1,2], J.-Z. LI[2], Q.-L. ZUO[2], C. LIU[1], H. JIANG[1], M.-Q. DU[1]

[1]MOST KLOS & KLOBM, School & Hospital of Stomatology, Wuhan University, Wuhan, China
[2]Affiliated Stomatological Hospital, Xiamen Medical College, Xiamen, China

Abstract. – OBJECTIVE: Infiltration resins provide an ideal treatment alternative for white spot lesions on teeth. The icon infiltrant has been widely used as a dental material for a few years, but there are some studies on the *in vitro* accelerated aging process and the change of hardness and microstructure on this material. The innovation of this work is to aim at investigating characteristics associated with this infiltrant resin and comparing the Icon infiltrant with universal Filtek Z350 and flowable Filtek Z350 resins when exposed to artificial accelerated aging.

MATERIALS AND METHODS: Materials were prepared as disc-shaped specimens sized to 12 mm × 2.2 mm and were aged through exposure to 150 kJ/m^2 in an artificial accelerated aging machine. Two-time points, 24 h after aging and 96 h after aging, were selected for evaluation in the following trials. The morphology was observed using a scanning electron microscopy. The standard CIEL*a*b* color system was employed for color measurements. Microhardness of all specimens was analyzed by a Knoop indenter. Chemical components were examined by Fourier transform infrared spectroscopy.

RESULTS: Compared with universal Z350 and flowable Z350, the ICON infiltrant resin presented a uniform, slightly scratched surface before and after accelerated aging. The 24 h artificial accelerated aging of the three investigated materials resulted in acceptable color alterations, a ΔE* range of 2.52±0.63 for universal Z350, 2.43±0.59 for flowable Z350 and 3.31±0.32 for ICON. After 96 h aging, significant color changes were noted for universal Z350 (7.51±0.63) and ICON (4.70±0.69). The ICON infiltrant displayed reduced microhardness when compared to universal Z350 and flowable Z350. The absorption peaks of the chemical bonds were significantly altered after the accelerated aging process.

CONCLUSIONS: Composed in a triethylene glycol dimethacrylate (TEGDMA) monomer-based network, the color stability and microhardness of the infiltrant resin provided suitable material for treating white spot lesions (WSLs), yet presented susceptibility under accelerated aging. Thus, osmotic resin therapy has strict limitations to be most effective.

Key Words:
Resin infiltrant, Accelerated aging, Microhardness, Microstructure.

Introduction

While general oral hygiene has been popularized over the past century, the prevalence of enamel caries or more commonly, tooth decay, remains high. An early enamel lesion is characterized by decalcification under the intact enamel, while white spot lesions (WSLs) provide the initial clinical manifestation of the enamel decay[1]. WSLs propagate due to the accumulation of organic acids produced by bacteria, which hinder the balance of the essential demineralization and remineralization process. Continuous demineralization results in a loss of calcium ions and an increase in porosity. This porous layer alters the reflective index of enamel and permits further bacteria colonization.

To prevent carious development, either invasive or noninvasive procedures are employed. Researchers have preferred a noninvasive strategy for early enamel lesions, such as remineralization[2]. Common treatments include fluoride therapy, casein–phosphopeptide-amorphous calcium phosphate (CPP-ACP) pastes, or laser therapy. However, fluoride treatments are confined to the surface of the lesion, unable to penetrate deeper into the enamel and the de-

Corresponding Author: Minquan Du, MD; e-mail: duminquan@whu.edu.cn

mineralized tissue. Chansley and Kral[3] further propose that the long-term effects of fluoride applications likely result in the expansion of drug-resistance bacteria. Therefore, the infiltration treatment method proposed in the early 1970s was an effort to avoid the risks associated with noninvasive strategies.

Various infiltration reagents have been studied, namely adhesives, fissure sealants, and infiltration resins as a treatment method of WSLs[4]. Specifically, infiltration resins for WSLs were identified as a microinvasive treatment option, balancing both operative and nonoperative methods[5,6], without destruction of the normal tooth structure.

In a recent investigation, a WSLs prevalence of 46-73% was reported in patients possessing a form of fixed orthodontic therapy[7]. Cazzolla et al[8] applied an ICON resin infiltration to orthodontic-induced WSLs. Collected data indicated that neither the color of the ICON infiltration nor the aesthetic camouflage was altered after 4 years of exposure to the oral environment. Compared with NaF and bioactive glass, the ICON infiltration resin performed more effectively in treating WSLs and returning the enamel to its natural color[6]. When penetrated with ICON resin (refractive index, RI=1.42), which possesses a similar RI as a sound enamel, the resulting RI of the treated WSLs was similar to normal, resulting in lesions with a natural appearance. Additionally, ICON is a unique resin since it has the component of triethylene glycol dimethacrylate (TEGDMA), which could inhibit the progression of caries upon their infiltration into the porous enamel layer[9].

Although ICON resin has the advantages of masking WSLs and preventing caries lesions, several investigations have focused on the mechanical properties after ICON infiltration[5]. When compared to composites and flowable resins, ICON resin provides increased permeability and decreased hardness. The ICON infiltrant could be used to recover the hardness both in the superficial enamel and in that of the underlying enamel. However, the altered mechanical properties of the ICON resin are not ideal for cavity caries. There remains a lack of comprehensive evaluations of accelerated aging effects on color, hardness, and microstructure of the ICON resin compared to traditional resins. Therefore, the present study aims to investigate the stability of these characteristics after exposure to an artificial aging technique.

Materials and Methods

Sample Preparation

Two types of composite resins were evaluated: a traditional composite resin (universal Filtek Z350, 3M, USA) and a conventional flowable resin (Filtek Z350, 3M, USA). The resin infiltrant used was ICON (DMG, Hamburg, Germany). The related characteristics are listed below in Table I.

For each group, seven plastic disc-shaped composite specimens were fabricated using polytetrafluoroethylene (PTFE) cylindrical molds, measuring 12 mm in diameter and 2.2 mm thickness. The resin materials were transferred into the molds, sealed with polyester films, and then pressed between two glass slides. For all specimens, each surface was irradiated for 20 s using the light LED unit (SLC VIIIc, Hangzhou, China), with six contiguous regions on each side. All samples were then polished using 1500- and 2000-grit SiC paper (Allied High Tech Products Inc. Compton, CA, USA), and finished under cooling water to a thickness of 2.00 ± 0.05 mm. Thereafter, the specimens were stored in a 37° C thermostatic machine for 24 h (SSW-600-2S Boxun Company, Shanghai, China).

Samples were aged through exposure to 150 kJ/m^2 using an artificially accelerated aging technique. The ISO 7491[10] standard for composite resin aging experiments is in a (37 ± 5) °C circulating water bath, fully exposed to a 150,000 Ix xenon arc lamp with irradiation for (24 ± 1) h. The power of a 150,000 Ix xenon arc lamp is equivalent to 662.25 W/m^2, and the total radiant energy for (24 ± 1) h irradiation is (57 218.4 ± 2 384.1) kJ/m^2. The Suntest CPS+ type aging instrument (xenon lamp aging instrument) used in this investigation has a total radiant energy of 56,160 kJ/m^2 for 24 h and a total radiation of 224, 640 kJ/m^2 for 96 h. The natural weather conditions of Miami, FL, USA in 2006. In the aging experimental field, the total energy of 45 degree's solar radiation is 6 199.8 MJ/m^2 and the average solar radiation energy is 16.985 75 MJ/m^2. Taking this as a standard, the radiation energy of the Suntest CPS+ type aging instrument for 24 h is equivalent to the radiation amount of 3.3l d of the natural weather condition aging test field in Miami, FL, in 2006, and the radiation energy of 96 h is equivalent to 13.23 days of radiation amount.

Table I. Restorative materials selected and characteristic composition.

Materials	Category	Manufacturer	Composition	Shade	Filler content (vol. %)
Filtek™ Z350 XT	Universal Restorative	3M ESPE, St. Paul, MN, USA	Nanofilled resin bis-GMA, UDMA, bis-EMA, TEGDMA, PEGDMA, and consisting of non-agglomerated/non-aggregated 20 nm silica filler, non-agglomerated/non-aggregated 4 to 11 nm zirconia filler, and aggregated zirconia/silica cluster filler	A2	63.3
Filtek™ Z350 XT	Flowable Restorative	3M ESPE, St. Paul, MN, USA	Microhybrid resin bis-GMA, bis-EMA, TEGDMA and consisting of fillers with a range of particles sizes from 0.1 to 5microns non-agglomerated/non-aggregated surface modified 20 nm and 75 nm silica filler, and surface modified aggregated zirconia/silica cluster filler	A2	46
ICON®	Infiltrant	DMG	TEGDMA, bis-GMA, initiators		0

bis-GMA = bis-phenol A diglycidylmethacrylate; UDMA = urethane dimethacrylate; bis-EMA = bis-phenol A polyetoxylated dimethacrylate; TEGDMA = triethyleneglycol dimethacrylate; PEGDMA = Polyethylene glycol dimethacrylate.

Measurement

Scanning Electron Microscopy (SEM, SU-70, Hitachi, Tokyo, Japan)

The micro-structures before and after accelerated aging were observed through Scanning Electron Microscopes (SEM) after surface coating. Micrographs were collected at 5 kV accelerating voltage and a working distance of 15 mm.

Color Measurement

The standard CIELab (Commission Internationale de I'Eclairage, France) color system was employed for color measurement using a reflection spectrophotometer (Color-Eye®7000, GretagMacbeth LLC, New Windsor, NY, USA). Measurements were collected across a visible spectrum range of 360-750 nm in increments of 10 nm. The spectrophotometer was calibrated before every process. A white background and standard illuminant with an area view of 8×12 mm aperture was used. The CIELab color space graph is a 3-D color measurement where CIE L represents the lightness coordinate ranging from 0 (extremely black) to 100 (extremely white), CIE a and CIE b axes refer to green-red (−a = green; +a = red) and blue-yellow (−b = blue; +b = yellow) chromaticity coordinates. Colorimetric values of the three groups before were determined as a baseline prior to the initiation of accelerated aging. The color difference (ΔE*) was calculated with the following formula:

$$\Delta E^* = [(\Delta L^*)^2 + (\Delta a^*)^2 + (\Delta b^*)^2]^{1/2}$$

(Equation 1)

in which ΔL^*, Δa^*, Δb^* refer to value differences between the baseline and aging times (24 h or 96 h), respectively. An elevated ΔE* indicates the lower color stability.

Hardness Analysis

The hardness of all specimens was analyzed by a Knoop indenter (HMV-2000; Shimadzu, Kyoto, Japan) with a load of 100 g and application of 10 s. For every irradiated surface, five hardness measurement parameters were evaluated. The averages of these data were defined as the Knoop hardness number (KHN, kgf/mm^2). Knoop hardness number (KHN) was calculated at baseline and 24 h or 96 h after artificial aging. The decrease in hardness between different time periods was recorded for analysis.

FTIR Analysis

Chemical properties before and after artificial aging at 24 h and 96 h were examined by Fourier transform infrared spectroscopy (FTIR, NICOLET iS10; Thermo Fisher Scientific, Waltham, MA, USA). Infrared spectra were recorded under the following conditions: DGTS detector with a resolution of 4 cm^{-1} (with 40-time scans), 400-4000 cm^{-1} wave number range, 2 µm depth of analysis at 1000 cm^{-1} and a 25 ±1°C chamber temperature. The following representative peak heights were recorded: -OH stretching vibrations at approximately 3150-3550 cm^{-1}, Si-O-Si stretching vibrations at approximately 1000-1100 cm^{-1} (for the fillers), $-CH^3$ asymmetric stretching vibrations at approximately 2958 cm^{-1}, and C-O stretching vibrations at approximately 1000-1300 cm^{-1}.

Statistical Analysis

The data are presented as mean values ± SEM and were statistically analyzed by a *t*-test and one-way ANOVA analysis. Differences between groups were considered significant when $*p < 0.05$, $**p < 0.01$, $***p < 0.001$ and $****p < 0.0001$. Statistical analyses were performed using GraphPad Prism (GraphPad Software, San Diego, CA, USA).

Results

SEM imaging was performed on each type of resin sample after exposure to accelerated aging techniques to investigate the resulting morphology, as shown in Figure 1. Baseline samples of universal Filtek Z350 and flowable Filtek Z350 (0 h aging), exhibited light and deep scratches, as well as filler protrusion. While, a uniform, moderately scratched surface was illustrated in the ICON baseline sample. After 24 h of artificial accelerated aging, deep pits and filler protrusions were more evident in the flowable Filtek Z350 resin, whereas uniform scratched surfaces remained in the universal Filtek Z350 resin. ICON samples displayed light scratches after a 24 h aging treat-

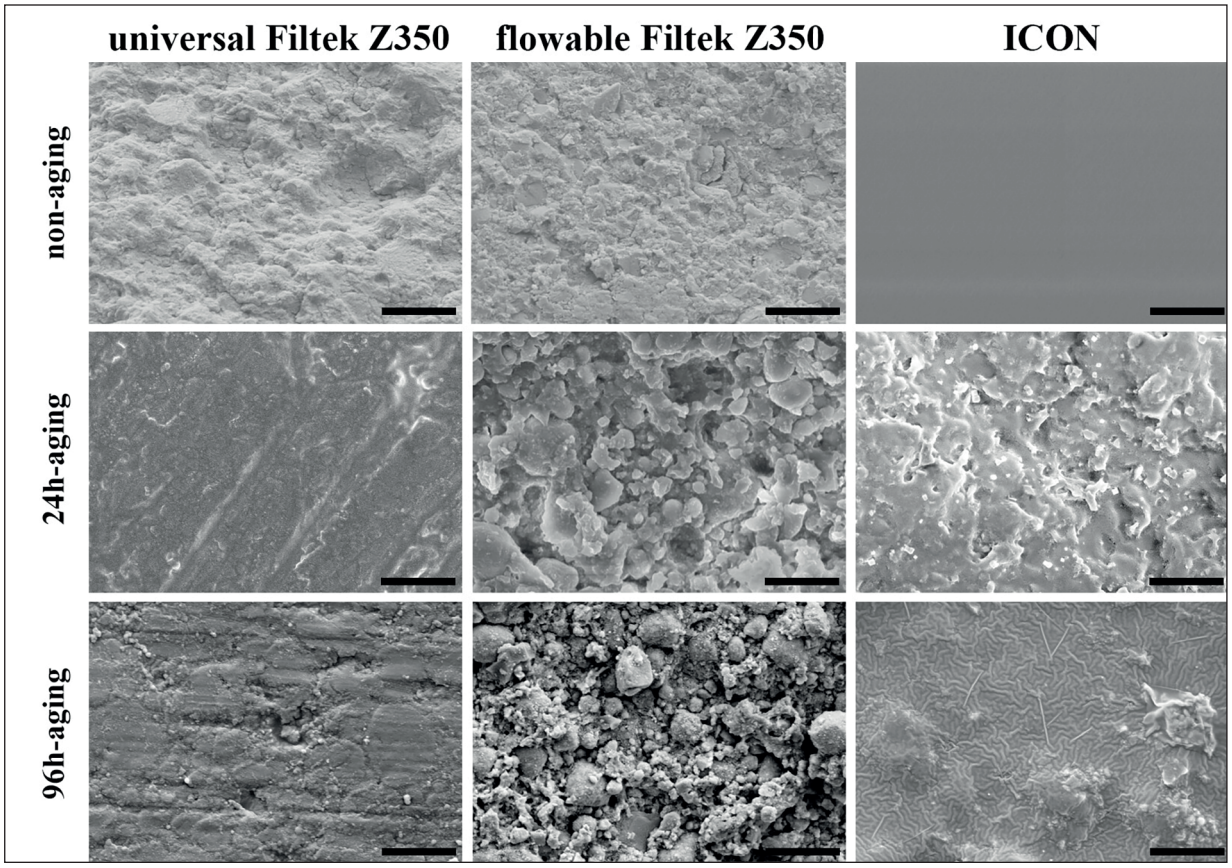

Figure 1. SEM scanning images of universal Filtek Z350, flowable Filtek Z350, and ICON, before and after accelerated aging (24 h and 96 h aging). Scale bar denotes 10 µm.

ment. After 96 h of artificial accelerated aging, a homogenous surface morphology was observed in both universal Filtek Z350 and ICON resins, while flowable Filtek Z350 maintained a deeply scratched surface with filler protrusions. As compared with universal Z350, ICON resins resulted in a more uniform surface post-aging treatment.

Color measurements were collected and presented as means and SDs of L*, a*, and b* values, before and after the accelerated aging. The color variation for each resin was calculated as ΔL*, Δa*, Δb*, as referenced to the color profile prior to treatment. All results from the color measurements are listed in Table II. Results indicate that the ΔL* range of universal Filtek Z350, flowable Filtek Z350, and ICON samples all differed after 24 h of aging. Measurements collected after 96 h of aging, demonstrate that both universal Filtek Z350 and flowable Filtek Z350 tended toward darker values, while the ICON samples presented a lighter color variation.

The Δa*, which represented the red-green range, was 0.48 and 0.82 for universal Filtek Z350 after 24 h and 96 h aging, respectively. Similarly, the Δa* range was 0.93 and 1.04 for flowable Filtek Z350 after 24 h and 96 h aging, respectively. Both Filtek resins preferentially displayed a red trend. On the contrary, the ICON resin samples produced a green trend after accelerated aging, resulting in values of -0.39 for 24 h aging and -0.34 for 96 h aging.

The Δb* represented color variation in the blue-yellow range. The universal Filtek Z350 displayed a blue trend after 24 h aging and a yellow trend after 96 h aging. Both flowable Filtek Z350 and ICON samples resulted in a yellow trend after 24 h and 96 h artificial aging. Collectively, the ΔE* range demonstrated the total color variation. We observed that the ΔE* range was relatively smaller after 24 h of artificial aging, resulting in values of 2.52 for universal Filtek Z350, 2.43 for flowable Filtek Z350 and 3.31 for the ICON samples. It was concluded that long-term artificial aging, as measured after 96 h of treatment, would cause significant color change for micro hybrids, whereby resultant ΔE* values were 7.51, 2.25 and 4.7 for universal Filtek Z350, flowable Filtek Z350, and ICON, respectively.

Each resin was evaluated *via* the Knoop hardness test. The mean microhardness values and standard deviations for the three resins are presented in Table III. Compared with universal Filtek Z350 and flowable Filtek Z350, the ICON infiltrant produced a lower hardness value at all of the three-time points investigated, before treatment (11.05±0.90), after 24 h of accelerated aging (56.33±17.53), and after 96 h of accelerated aging (53.94±15.73), as compared to the Filtek resins. Hardness values increased significantly ($p<0.05$) for the ICON resins after 24 h of treatment, as compared to the baseline ICON hardness values. However, no significant hardness differences were noted for either universal Filtek Z350 or flowable Filtek Z350. Over the course of the prolonged aging time of 96 h, it was found that flowable Filtek Z350 showed a significant increase in the hardness number ($p<0.01$). Of note, the ICON infiltrant demonstrated an enhanced hardness after a 96 h treatment regimen, as compared to the baseline, but it did not vary significantly from the hardness measured after the 24 h treatment period. These results suggested that the universal composite resins maintained a stable hardness throughout the accelerated aging treatment process. However, the ICON resin samples were more responsive to the accelerated aging timeline resulting in changes in hardness, which could end up in a significant difference in material properties long-term.

The FTIR investigation provided information regarding the chemical makeup of resins before and after the accelerated aging. FTIR spectral comparison of universal Filtek Z350, flowable Filtek Z350, and the ICON infiltrant before or af-

Table II. Means and SDs for differences in ΔL*, Δa*, Δb* before and after accelerated aging.

Materials	Aging period	ΔL*	Δa*	Δb*	ΔE*
Universal Filtek Z350	24 h	0.42 ± 0.17	0.48 ± 0.14	-2.83 ± 0.23	2.52 ± 0.63
Flowable Filtek Z350	24 h	-0.85 ± 0.43	0.93 ± 0.18	2.17 ± 0.78	2.43 ± 0.59
ICON	24 h	2.02 ± 0.72	-0.39 ± 0.07	2.64 ± 0.81	3.31 ± 0.32
Universal Filtek Z350	96 h	-3.07 ± 0.38	0.82 ± 0.32	6.98 ± 0.57	7.51 ± 0.63
Flowable Filtek Z350	96 h	-1.2 ± 0.42	1.04 ± 0.26	1.09 ± 0.29	2.25 ± 0.33
ICON	96 h	1.85 ± 1.38	-0.34 ± 0.14	3.62 ± 0.97	4.70 ± 0.69

ΔE* were calculated *via* $\Delta E^* = [(\Delta L^*)^2 + (\Delta a^*)^2 + (\Delta b^*)^2]^{1/2}$.

Table III. Hardness differences before and after accelerated aging.

Materials	Baseline	Aging period			
		24 h	24 h *vs.* baseline	96 h	96 h *vs.* baseline
Universal Filtek Z350	130.26 ± 13.72	146.31 ± 39.77	$p > 0.05$	258.21 ± 96.16	$p > 0.05$
Flowable Filtek Z350	113.84 ± 53.00	131.53 ± 32.78	$p > 0.05$	246.34 ± 18.58	$p < 0.01$
ICON	11.05 ± 0.90*	56.33 ± 17.53*	$p < 0.05$	53.94 ± 15.73**	$p < 0.05$

*Represented differences within columns *via* the one-way ANOVA analysis among universal Filtek Z350 and flowable Filtek Z350 and ICON at each tested time point (Baseline, 24 h aging, 96 h aging), with *$p < 0.05$, **$p < 0.01$. 24 h *vs*. Baseline, 96 h *vs*. baseline: *t*-test analysis within rows for comparison of universal Filtek Z350, flowable Filtek Z350, and ICON before or after aging.

ter artificial aging are shown in Figure 2. The related stretching vibrations are listed in Table IV. The resulting absorption peaks were significantly altered during the accelerated aging process, as attributed to the transformation of chemical groups. The universal Z350 resin demonstrated minimal chemical alteration when compared to

Table IV. The characteristic peaks of FTIR assignments.

Wave No. (cm^{-1})	Chemical groups	Strength
3150-3550	-OH stretching	Strong
1000-1100	Si-O-Si stretching	Strong
2958	-CH3 asymmetric stretching	Medium
1000-1300	C-O stretching	Strong

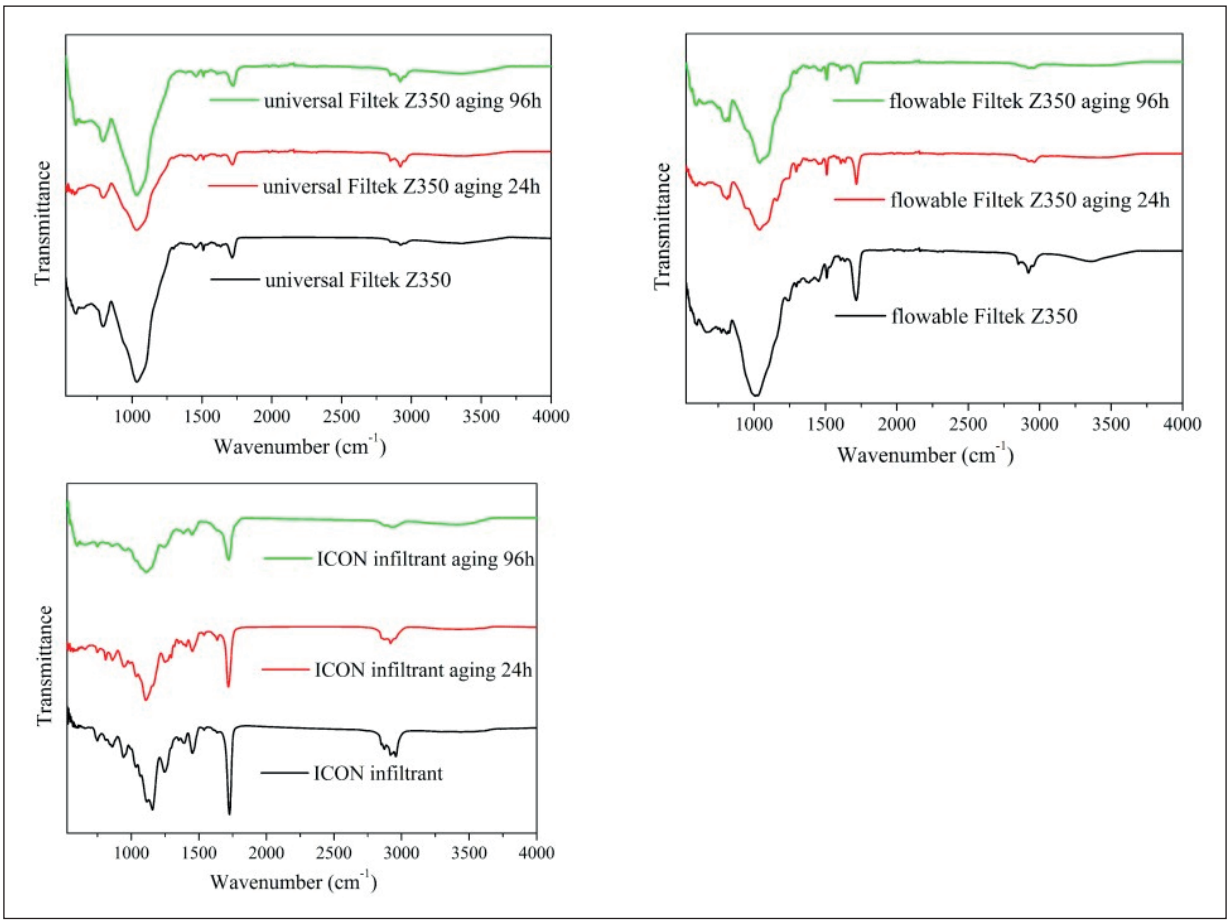

Figure 2. Alterations of functional groups, before and after aging (24 h and 96 h), as evaluated by FTIR.

the other tested resins. The stretching peaks at 1008 cm^{-1} indicating Si-O-Si groups were noted in the universal Z350 and flowable Z350. The detection of C-O peaks at 1000-1300 cm^{-1} was found in the ICON infiltrant. Moreover, the 3500 cm^{-1} vibrations of -OH in the ICON resin resulted from the aging treatment.

Discussion

Infiltration therapy was first introduced by Davila et al[11] in the 1970s. They found that the infiltrant could penetrate into the interior of demineralized enamel. Infiltrants, like pit and fissure sealants and resin binders, have been used to treat WSLs[12]. Despite the fact that these types of infiltrants could postpone the process of enamel demineralization, research indicates that the pit and fissure sealant or binder can only partially penetrate into the demineralized enamel. Treatment efficacy is therefore far from satisfactory. In contrast, the infiltration resin provides the following advantages: (1) an increase in the stability of the demineralized section; (2) the ability to preserve the healthy tooth and the physiological morphology; (3) means to permanently block micropore formation in the demineralized enamel; (4) the capacity to hinder caries progression; (5) postponement of filling treatments to minimize the risk of secondary caries; (6) improvement of the aesthetics of WSL; and (7) a minimally invasive and painless procedure for patients.

Like other resin materials, the infiltrant resin also inevitably faces problems including color variation and accelerated aging when exposed to the complex oral environment. Previous i*n vitro* studies have monitored the color variation of the lesion area after exposure to exogenous pigments, such as coffee and red wine. In those treated zones, it was found that the variation in color was significantly less in experimental groups than that seen for untreated groups. Furthermore, limitations in color variation with infiltrant resins were more effective with additional polishing[13]. The color and brightness of the lesion area were improved more effectively when treated with infiltrant than remineralization therapy[14]. It has also been suggested that during the infiltration treatment, the excess penetrant should be removed before curing to reduce the roughness of the infiltrated enamel lesions[15].

In the present work, the effects of accelerated aging on infiltrant resin were evaluated *via* the change of color, hardness, and chemical components. The UV-accelerated aging process monitor mimics the oral environment by modulating long-term effects of temperature and humidity changes on materials[16]. It was previously reported that 300 h of exposure to artificial UV-accelerated aging could simulate 24-months of clinical variations in an oral environment[17]. Treated with UV-irradiation, materials underwent internal reaction without outside stain influence.

The timely observation of surface morphology of the resin materials using scanning electron microscopy (SEM) remains a common method for evaluating roughness, porosity and cracks after exposure to UV irradiation[18,19]. The present study monitored the surface alterations of the three resins presented within. As was expected, the ICON infiltrant displayed the most uniform surface before aging. Despite small scratch formations after 24 h aging, the surface remained smooth until 96 h aging. Research suggests that UV aging can cause a loss of cohesion between particle fillers, thus leading to a physical surface modification[20]. However, pores and microcracks on the material surface prove susceptible to plaque accumulation and increased risk for secondary caries. According to literature, a surface roughness value under 0.2 μm is required for the restorative materials[20].

Moreover, the ICON resin possesses a permeability coefficient more suitable for repairing the junction between the resin and the demineralized enamel, as compared with the other two resins. Paris et al[22] found infiltration resins in enamel defects with a permeability coefficient of 273 cm/s and resulted in significantly greater penetration depths than that of a binder with a permeability coefficient of 31 cm/s. Paris et al[2] demonstrate that the permeability of resin is highly influenced by the air accumulation in the micropores, the organic smear layer on the lesion surface, and the presence of uneven pores in the demineralized enamel. Additive ethanol and TEGDMA in the ICON resin could significantly reduce the viscosity and the contact angle of the material, thereby increasing the permeability coefficient. Thus, these properties enhanced the effectiveness of the infiltrant resin through decreased morbidity, microleakage, and secondary caries.

The present work used the standard CIE L*a*b* system to measure the color alterations. The L*a*b* color system developed by CIE employs three values to describe the color index of the observed materials i.e., CIE L of light-dark, CIE a of green-red, and CIE b of blue-yellow. In

the present research at both 24 h and 96 h of accelerated aging, the ICON resin displayed higher values of ΔL than the other two resins, suggesting that ICON is visualized as a lighter material. Compared to universal Filtek Z350 and the ICON infiltrant, flowable Filtek Z350, a flowable resin, possessed a higher value of Δa at both test points, indicating a red tendency after the accelerated aging. All the three resins exhibited statistically significant color alteration after 24 h and 96 h aging. Previous studies[23,24] have demonstrated a clinically acceptable discoloration, ΔE value (ΔE<3.3), as a threshold. The three resins investigated herein exhibited acceptable color changes within this range after 24 h of accelerated aging. However, after 96 h of accelerated aging, the universal Filtek Z350 restorative resin and the ICON infiltrant experienced significant discoloration beyond the threshold in contrast to the flowable Filtek Z350. Overall, the ICON infiltrant exhibited less color change (ΔE=4.70±0.69) relative to the universal Filtek Z350 (ΔE=7.51±0.63).

Inokoshi et al[25] have identified the essential effectiveness of a matrix as related to the color stability of resins. The universal matrix in resins, including TEGDMA, bisphenol A-glycidyl methacrylate (bis-GMA), and a fraction of urethane dimethacrylate (UDMA) in the bis-GMA/TEGDMA co-monomer is reported to reduce water absorption and color changes[26]. Thus, the ICON infiltrant, composed of TEGDMA, exhibited color changes after 96 h of aging. We observed the highest ΔE values in the universal Filtek Z350, likely attributed to the filler size in the material. According to previous studies[27], water uptake alone could not account for the color changes, but the large size of fillers increased color susceptibility. Thus, the factors influencing color stability were not confined to matrix composition, but also included filler volume, pigment, and other activators or inhibitors[28]. Incorporation of a greater concentration of TEGDMA has been shown to improve the permeability coefficient as noted in the ICON infiltrant, while also potentially increasing polymerization shrinkage, brittleness, and solubility in saliva, thus reducing color stability. In the present report, the ICON infiltrant possessed a uniform surface, as observed *via* SEM, with slight color changes as reported by the CIE L*a*b* system, with CIE Δb accounting for the majority of the changes.

During the clinical application for enamel restoration, the various types of resins must withstand a complex oral environment, which includes harsh pH in saliva, temperature alterations, humidity, and mechanical stresses[29]. The present study investigated the microhardness of the three resins to evaluate the wear resistance of these materials. At both the 24 h and 96 h aging points, the nano-filled universal Filtek Z350 exhibited higher quantitative values than flowable Filtek Z350, though not statistically significant. These results were in accordance with those collected by Da Silva et al[30]. It was reported that filler components and morphology of the resins influenced mechanical properties[31]. Both the two resins possessed the following components including bis-GMA, bis-EMA, TEGDMA, and additive zirconia/silica particles. The relatively greater hardness of flowable Filtek Z350 and universal Filtek Z350, as compared with the ICON infiltrant is likely due to the presence of zirconia particles. Compared with the baseline time point (11.05±0.90), the hardness of the ICON infiltrant increased significantly both at 24 h (56.33±17.53, $p<0.05$) and 96 h (53.94±15.73, $p<0.05$). However, the ICON infiltrant presented the lowest hardness value changes when compared to the universal Z350 and flowable Z350.

The main addition of hydrophilic TEGDMA in the resin results in a dilution of the viscous structure of Bis-GMA, but inevitably leads to increased water uptake and reduced mechanical properties. Other monomers have been used to improve the defects of a Bis-GMA based system. With lower viscosity and higher flexural strength, UDMA copolymers were introduced into the present resin components. Previous studies[32,33] found that TEGDMA possesses the densest polymer network with the highest water absorption rate, while bis-GMA created the most rigid network with a moderate water absorption rate as compared to TEGDMA and UDMA. Therefore, it is reasonable to conclude that materials containing TEGDMA result in higher water absorption and solubility than those materials with Bis-GMA and UDMA[34]. Unlike universal Filtek Z350 and flowable Filtek Z350, the ICON infiltrant possessed a polymer network mainly consisting of TEGDMA. This composition is likely to lead to lower hardness properties for the ICON infiltrant. Therefore, the ICON infiltrant is most suitable for the treatment of WSL, an early enamel lesion, as opposed to already formed cavities.

The chemical composition and functional groups of the three resins were investigated using FTIR *via* absorbance mode. The accelerated aging process might lead to monomer dilution,

among the above-mentioned monomers, TEGDMA has been identified to be released faster than other monomers[20]. Monomer leaching is greatly affected by a number of factors including filler proportion, type of monomer, and chemical constitution of the resin. As demonstrated in the FITR spectra, the absorption peaks of the resins were significantly altered during the accelerated aging process, which was mainly attributed to the transformation of chemical groups. Among the three resins, the components of the universal Z350 were minimally altered, as in accordance with the measured hardness variation. The addition of silicon in the universal Z350 and flowable Z350 was found in Si-O-Si groups stretching peaks at 1008 cm^{-1}. The detection of C-O peaks at 1000-1300 cm^{-1}, representing ester groups, was related to the chemical makeup of TEGDMA in the ICON infiltrant. Moreover, the 3500 cm^{-1} vibrations of -OH in the ICON resulted from the accelerated aging process, possibly indicating hydrolysis of monomers, fracture of ester bonds or penetration of water in the polymers[35]. Therefore, the reduced content of TEDGMA and even the minimal content of the UDMA monomer in universal Z350 and flowable Z350 was accounted for in the inconspicuous peaks of -OH. The previously mentioned chemical degradation or water absorption in monomers might affect the integration of resins with the hard tissues of teeth. However, the underlying mechanism requires further investigation due to the complexity of the resins studied.

Conclusions

We showed that infiltrant resins have been a preferred method of treating early enamel lesions due to their refractive index similar to normal enamel, low viscosity, and high permeability. Infiltrants can easily penetrate into the microporous structure of demineralized enamel, thereby recovering a uniform enamel surface, inhibiting the progress of early stage caries and providing partial mechanical properties for dental tissues. However, coupled with a TEGDMA monomer-based network, the color stability and microhardness of the infiltrant resin might be susceptible to accelerated aging. It remains imperative for further investigation to determine the proper ratio of monomer networks to optimize color stability, mechanical properties, and effective treatment of early enamel lesions with the preferred infiltrant resins. Ultimately, osmotic resin therapy has strict limitations and indications for use. The infiltrated resin can penetrate into demineralized enamel, but cannot fill the formed cavities. Therefore, the infiltrating resin is only suitable for unformed cavities and lesions confined to the enamel surface or upper third of the dentin, which are located at or adjacent to the smooth surface of a tooth.

Conflict of Interest

The Authors declare that they have no conflict of interests.

References

1) Julien KC, Buschang PH, Campbell PM. Prevalence of white spot lesion formation during orthodontic treatment. Angle Orthod 2013; 83: 641-647.
2) Kantovitz KR, Pascon FM, Nobre-dos-Santos M, Puppin-Rontani RM. Review of the effects of infiltrants and sealers on non-cavitated enamel lesions. Oral Health Prev Dent 2010; 8: 295-305.
3) Chansley PE, Kral TA. Transformation of fluoride resistance genes in Streptococcus mutans. Infect Immun 1989; 57: 1968-1970.
4) Kim S, Kim EY, Jeong TS, Kim JW. The evaluation of resin infiltration for masking labial enamel white spot lesions. Int J Paediatr Dent 2011; 21: 241-248.
5) Freitas MCCA, Nunes LV, Comar LP, Rios D, Magalhães AC, Honório HM, Wang L. In vitro effect of a resin infiltrant on different artificial caries-like enamel lesions. Arch Oral Biol 2018; 95: 118-124.
6) Prasada KL, Penta PK, Ramya KM. Spectrophotometric evaluation of white spot lesion treatment using novel resin infiltration material (ICONR). J Conserv Dent 2018; 21: 531-535.
7) Knösel M, Eckstein A, Helms HJ. Long-term follow-up of camouflage effects following resin infiltration of post orthodontic white-spot lesions in vivo. Angle Orthod 2019; 89: 33-39.
8) Cazzolla AP, De Franco AR, Lacaita M, Lacarbonara V. Efficacy of 4-year treatment of icon infiltration resin on postorthodontic white spot lesions. BMJ Case Rep 2018; 2018. pii: bcr-2018-225639.
9) Inagaki LT, Alonso RC, Araújo GA, de Souza-Junior EJ, Anibal PC, Höfling JF, Pascon FM, Puppin-Rontani RM. Effect of monomer blend and chlorhexidine-adding on physical, mechanical and biological properties of experimental infiltrants. Dent Mater 2016; 32: e307-e313.
10) Dental Materials: determination of colour stability. International Organization for Standardization 2000.

11) Davila JM, Buonocore MG, Greeley CB, Provenza DV. Adhesive penetration in human artificial and natural white spots. J Dent Res 1975; 54: 999-1008.

12) Rocha Gomes Torres C, Borges AB, Torres LM, Gomes IS, de Oliveira RS. Effect of caries infiltration technique and fluoride therapy on the colour masking of white spot lesions. J Dent 2011; 39: 202-207.

13) Paris S, Schwendicke F, Keltsch J, Dorfer C, Meyer-Lueckel H. Masking of white spot lesions by resin infiltration in vitro. J Dent 2013; 41 Suppl 5: e28-34.

14) Cohen-Carneiro F, Pascareli AM, Christino MR, Vale HF, Pontes DG. Color stability of carious incipient lesions located in enamel and treated with resin infiltration or remineralization. Int J Paediatr Dent 2014; 24: 277-285.

15) Mueller J, Yang F, Neumann K, Kielbassa AM. Surface tridimensional topography analysis of materials and finishing procedures after resinous infiltration of subsurface bovine enamel lesions. Quintessence Int 2011; 42: 135-147.

16) Douglas RD. Color stability of new-generation indirect resins for prosthodontic application. J Prosthet Dent 2000; 83: 166-170.

17) Powers JM, Fan PL, Raptis CN. Color stability of new composite restorative materials under accelerated aging. J Dent Res 1980; 59: 2071-2074.

18) Schulze KA, Marshall SJ, Gansky SA, Marshall GW. Color stability and hardness in dental composites after accelerated aging. Dent Mater 2003; 19: 612-619.

19) Wozniak WT, Moser JB, Willis E, Stanford JW. Ultraviolet light stability of composite resins. J Prosthet Dent 1985; 53: 204-209.

20) Catelan A, Suzuki TYU, Becker F Jr, Briso ALF, Dos Santos PH. Influence of surface sealing on color stability and roughness of composite submitted to ultraviolet-accelerated aging. J Investig Clin Dent 2017; 8 (2). doi: 10.1111/Jicd.12203. Epub 2016 Jan 8.

21) Paris S, Meyer-Lueckel H, Cölfen H, Kielbassa AM. Penetration coefficients of commercially available and experimental composites intended to infiltrate enamel carious lesions. Dent Mater 2007; 23: 742-748.

22) Paris S, Dörfer CE, Meyer-Lueckel H. Surface conditioning of natural enamel caries lesions in deciduous teeth in preparation for resin infiltration. J Dent 2010; 38: 65-71.

23) Kumbuloglu O, Lassila LV, User A, Vallittu PK. A study of the physical and chemical properties of four resin composite luting cements. Int J Prosthodont 2004; 17: 357-363.

24) Vichi A, Ferrari M, Davidson CL. Color and opacity variations in three different resin-based composite products after water aging. Dent Mater 2004; 20: 530-534.

25) Inokoshi S, Burrow MF, Kataumi M, Yamada T, Takatsu T. Opacity and color changes of tooth-colored restorative materials. Oper Dent 1996; 21: 73-80.

26) Kalachandra S, Turner DT. Water sorption of polymethacrylate networks: bis-GMA/TEGDM copolymers. J Biomed Mater Res 1987; 21: 329-338.

27) Dietschi D, Campanile G, Holz J, Meyer JM. Comparison of the color stability of ten new-generation composites: an in vitro study. Dent Mater 1994; 10: 353-362.

28) Korkmaz Ceyhan Y, Ontiveros JC, Powers JM, Paravina RD. Accelerated aging effects on color and translucency of flowable composites. J Esthet Restor Dent 2014; 26: 272-278.

29) Arslan S, Lipski L, Dubbs K, Elmali F, Ozer F. Effects of different resin sealing therapies on nanoleakage within artificial noncavitated enamel lesions. Dent Mater J 2018; 37: 981-987.

30) DA Silva. MA, Vitti RP, Sinhoreti MA, Consani RL, Silva-Júnior JG, Tonholo J. Effect of alcoholic beverages on surface roughness and microhardness of dental composites. Dent Mater J 2016; 35: 621-626.

31) Kim KH, Ong JL, Okuno O. The effect of filler loading and morphology on the mechanical properties of contemporary composites. J Prosthet Dent 2002; 87: 642-649.

32) Tanimoto Y, Hayakawa T, Nemoto K. Analysis of photopolymerization behavior of UDMA/TEGDMA resin mixture and its composite by differential scanning calorimetry. J Biomed Mater Res B Appl Biomater 2005; 72: 310-315.

33) Sideridou I, Tserki V, Papanastasiou G. Study of water sorption, solubility and modulus of elasticity of light-cured dimethacrylate-based dental resins. Biomaterials 2003; 24: 655-665.

34) Park J, Eslick J, Ye Q, Misra A, Spencer P. The influence of chemical structure on the properties in methacrylate-based dentin adhesives. Dent Mater 2011; 27: 1086-1093.

35) Yiu CK, King NM, Carrilho MR, Sauro S, Rueggeberg FA, Prati C, Carvalho RM, Pashley DH, Tai FR. Effect of resin hydrophilicity and temperature on water sorption of dental adhesive resins. Biomaterials 2006; 27: 1695-1703.